Thermodynamic Tri-Objective Optimisation of a Combined ORC-TFC Cycle for Low-Temperature Power Generation

Mohamed M. El-Awad

Independent researcher, P.O. Box 321 Khartoum, Sudan

Email: mmelawad09@gmail.com

ORCID: https://orcid.org/0000-0002-3951-4725

Tel: +2490125020773, +2490963151609

ABSTRACT: This paper presents a new cycle for utilising the energy from low-temperature heat sources that combines the Organic Rankine Cycle (ORC) with the Trilateral Flash Cycle (TFC) via a cascade condenser. The model developed for analysing the cycle uses Excel as a modelling platform with special VBA functions to determine the fluid properties. To verify the functions, they were used to analyse the simple OCR by using R134a, R1234yf, R152a, propane (R290), n-butane (R600), iso-butane (R600a), and ammonia (R717) and the model'sresults are compared with published results obtained by using the EES software. When the performance of the combined cycle was evaluated for a heat-source of 120°C at various values of the cascade-condenser temperature by using R152a as the working fluid, the results showed that a high temperature maximises the cycle's power and exergetic efficiency but minimises its thermal efficiency. Therefore, a tri-objective optimisation analysis of the cycle was conducted that simultaneously maximises all three parameters. Compared to the temperature that gives the maximum power, the optimised temperature reduced the power by 11.9%, but increased the thermal efficiency by 15.3% and the exergetic efficiency by 5.7%. Compared to the temperature that gives the maxmimum thermal efficiency, the optimised temperature reduced the thermal efficiency by only 5.9%, but increased the power by 68.8% and the exergetic efficiency by 4.3%.

Keywords: Low-temperature heat recovery, ORC, TFC, Excel, Thermax, MIDACO

One of the promising technologies for the utilisation of low and moderate temperature heat sources is the organic Rankine cycle (ORC) (Fierro et al., 2022; Wolf et al., 2023). Unlike the conventional Rankine cycle, the ORC does not require very high temperatures to apply and can adapt to low-temperature heat sources by using an organic fluid as the working fluid instead of steam. However, like the conventional cycle, the efficiency of the ORC deteriorates if the temperature of the heat source is reduced or that of the condenser is increased. Although various modifications to the simple ORC can be adopted for improving the cycle's efficiency, such as reheating, regeneration, and recuperation, these modifications do not address a main drawback of the ORC which is the mismatch between the temperature of the heating source and that of the working fluid during the heat-addition process in the evaporator (Skiadopoulos et al., 2023). A newly proposed cycle that can solve this problem is the trilateral flash cycle (TFC) in which the saturated liquid fluid is not allowed to vaporise during the heat recovery process but directly taken to expand in a two-phase expander (Yari et al., 2015; Skiadopoulos et al., 2023). Since the technology of TFC expanders is relatively immature compared to the conventional turbines, they are costlier and less efficient (Fierro et al., 2022, Yari et al., 2015).

Many previous researchers developed theoretical models for comparing the performance of the ORC and TFC from thermodynamics and thermoeconomic viewpoints or compared them with other cycles such as the Kalina cycle. For example, Bidgoli and Yanagihara (2023) analysed an ORC cycle that recovers the waste heat from the intercoolers of the compression units of a large processing plant. By using Aspen HYSYS (Aspen Plus, 1992) as the modelling platform, they analysed the cycle with various working fluids including R123, n-butane, n-pentane, hexane, and n-heptane. Their results showed that a net power of up to 40 MW could be generated with R123. Wolf et al. (2023) investigated a solar powered ORC by using a zeotropic iso-pentane/CO_2 mixture. Modelling of the system was done by using EES (Klein; Alvarado, 1992) and all thermodynamic properties were determined by using REFPROP (Lemmon et al., 2004). Their exergy and exergo-economic analyses showed that the investigated unit was capable of co-producing approximately 30 kW of electricity and 160 kW district heating with an exergetic efficiency exceeding 60%. They concluded that the unit was able to compete with existing renewable power generating systems in terms of specific cost of electricity.

Previous researchers also reported the results of theoretical studies of cascade ORC systems or hybrid systems involving ORC with steam turbines. For example, Oko et al. (2016) presented exergoeconomic analysis of a 100 kW solar driven ORC power plant. They considered a cascade cycle of R134a and R290 working fluids and developed their model in Microsoft Excel and MATLAB environments. They determined the energy and exergy efficiencies of the proposed plant, at the optimal collector operation, as 18.92 and 21.61%, respectively. The total capital investment, levelized cost of energy (LCOE), payback period and the earning power of the investment were estimated to be 352 US$/kW, 0.0072 US$/kWh, 2 years 7 months, and 14.3%, respectively. Najjar and Qatramez (2019) modelled a hybrid system consisting of a single flash geothermal cycle operating on a steam turbine and ORC using R600, R600a, R11, and R123. The highest efficiency of 18.76% and net power output of 24,887MW were obtained with R11. Mokarram and Mosaffa (2020), who studied a cycle that integrated a steam turbine and a trans-critical ORC with R245fa, showed that the system could produce 7.2% more power compared to a similar cycle operating in subcritical conditions. With a maximum energy and exergy efficiencies of 14.66% and 55.15%, respectively, the LCOE was 0.2018 US$/kWh.

The above literature review reveals that a cycle that combines the TFC in the high-temperature circuit (HTC) and the ORC in the low-temperature circuit (LTC) has not been considered before. This conclusion is also supported by the more comprehensive review given in (Jiménez-García et al., 2023). While minimising the mismatch between the working fluid and the heat source for the ORC, the new cycle enables different organic fluids to be used in the HTC and LTC that suit the high and low temperature ranges better than a single fluid and enables a turbine to be used in the LTC instead of the two-phase expander. The cycle also gives cogeneration systems more flexibility than a single ORC or LTC. The present paper contributes to knowledge by presenting thermodynamic evaluation and multi-objective optimisation of this new cycle. From another perspective, the above literature review shows that most researchers used commercial software for their analyses. However, the use of general-purpose software can encourage independent researchers and engineering students to contribute to the development of innovative ORC and TFC systems using environment-friendly fluids (Trædal, 2014; Oko and Diemuodeke, 2013). In this respect, the present paper uses Microsoft Excel as the modelling platform with special VBA functions to determine the thermodynamic properties of the working fluids while the free version of the MIDACO solver (Schlueter et al., 2012) is used for the multi-objective optimisation analysis.

MATERIALS AND METHODS

The combined ORC-TFC cycle

The ORC system has the same components as those of the conventional steam-turbine power plant which are the evaporator (boiler), the turbine, the condenser, and the pump. However, organic fluids are used in the ORC instead of water because they have higher boiling pressures at low temperatures. The TFC differs from the ORC by heating the working fluid without going into the vaporisation process so that the hot pressurised fluid expands in the two-phase region. By leading to a uniform temperature glide between the heat source and the working fluid, this cycle reduces the losses during the heat-transfer process and improves the performance of the system. Typically, TFC system can provide 50% more work than ORC system for the same energy input, but they need sophisticated expanders that can adequately handle the liquid-phase presence during the expansion process (Fierro et al, 2022). Apart from increasing the investment cost, two-phase expanders are less efficient than the turbines.

Figure 1.a shows a schematic diagram of the combined ORC-TFC system in which the heat source is first used to heat the working fluid of the TFC circuit and then to heat the working fluid of the ORC circuit. After expanding in the two-phase expander to produce power, the working fluid of the TFC circuit is condensed by the cooler working fluid of the ORC circuit in a cascade condenser (cc) and then pumped into the TFC heater. The ORC system shown on Figure 1.a is a recuperative system in which the superheated fluid exiting the turbine is used to heat the cold fluid exiting the pump in an internal heat-exchanger (IHEX). Accordingly, the initially superheated fluid exiting the turbine enters the condenser of the ORC as saturated vapour. In the condenser, the working fluid is cooled by the cooling water to the saturated-liquid state and then pumped into the cold side of the IHEX. After the IHEX, the fluid is heated by the heat source to the state of saturated liquid before entering the cascade condenser where it is heated by the condensing fluid of the TFC circuit until it becomes saturated vapour.

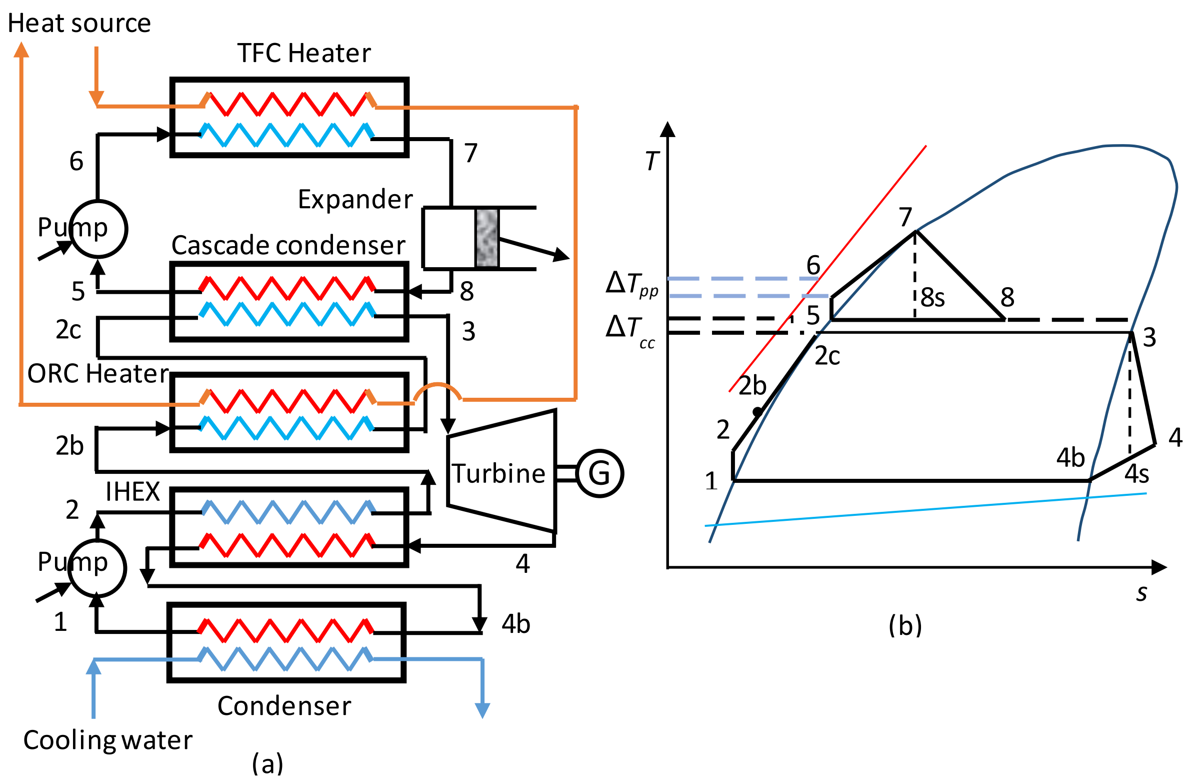

Figure 1. Schematic and *T-s* diagrams for the combined TFC-ORC cycle

Figure 1.b shows the *T-s* diagram of the combined system. Unlike the TFC cycle in which the pinch point occurs where the heating fluid exits the system, that of the combined cycle occurs in the middle of the heating process which forces the heating source to exit the system at a higher temperature than that of the TFC. Although this limits the amount of heat recovered and the work produced by the ORC circuit, the combined cycle can still produce more work than the simple ORC because of the additional work produced by the TFC circuit. Compared to the simple TFC, the combined cycle can have a higher thermal efficiency by allowing two different working fluids to be used in the TFC and ORC circuits that lead to a better overall performance and by replacing the two-phase expander with the single-phase turbine. As shown later, the power produced by the cycle and its thermal and exergetic efficiencies depend on the temperature of the cascade condenser. While the thermal efficiency increases by increasing this temperature, the cycle's power decreases and the exergetic efficiency has an optimum at a certain value. Therefore, determining the cascade temperature that gives the desired trade-off between the three performance indicators poses a tri-objective optimisation problem.

The analytical models for the TFC and ORC circuits and the combined cycle

The analytical model for thermodynamic analyses of the cycle assumes steady-state operation and neglects pressure losses and heat-transfer losses in the various components. However, the losses due to irreversibility in the pumps, the turbine, and the two-phase expander are taken into consideration via the relevant the isentropic efficiencies (Moran; Shapiro, 2006).

The analytical model for the TFC circuit

Given the pinch-point temperature difference, ΔT_{pp}, the temperature of the heat source exiting the TFC heater, $T_{hso,TFC}$, is determined from:

$$T_{hso,TFC} = T_6 + \Delta T_{pp} \qquad (1)$$

Given the inlet temperature of the heat source, $T_{hs,in}$, and its mass flow rate, $\dot{m}_{hs}$, the rate of heat transfer from the heat source (assumed to be a stream of hot-water) to the working fluid of the TFC, $\dot{Q}_{hs,TFC}$, and the mass flow rate of the working fluid, $\dot{m}_{TFC}$, are calculated from:

$$\dot{Q}_{hs,TFC} = \dot{m}_{hs} c_p \left(T_{hs,in} - T_{hso,TFC}\right) \qquad (2)$$

$$\dot{m}_{TFC} = \dot{Q}_{hs,TFC} / \left(h_7 - h_6\right) \qquad (3)$$

The specific work,in kJ per kg,of the TFC pump is given by:

$$w_{p,TFC} = v_5 \left(p_{heater,TFC} - p_{cc,TFC}\right) / \eta_{p,TFC} \quad (4)$$

Where $p_{heater,TFC}$ and $p_{cc,TFC}$ are the pressures of the TFC fluid in the heater and cascade-condenser, respectively, and $\eta_{p,TFC}$ is the isentropic efficiency of the TFC pump. Equation (5) is then used to determine the enthalpy of the fluid at state 6 after the pump:

$$h_6 = h_5 + w_{p,TFC} \qquad (5)$$

The specific work of the working fluid in the TFC during the two-phase expansion process is evaluated from the enthalpy change as follows:

$$w_{exp} = \left(h_7 - h_{8s}\right) \times \eta_{exp} \qquad (6)$$

Where η_{exp} is the isentropic efficiency of the expander and h_{8s} is the enthalpy of the fluid after an isentropic expansion (refer to Figure 1.b). The thermal efficiency of the TFC circuit alone is given by:

$$\eta_{TFC} = \dot{m}_{TFC} \left(w_{exp} - w_{p,TFC}\right) / \dot{Q}_{hs,TFC} \qquad (7)$$

The analytical model for the ORC circuit

The mass flow rate of the working fluid in the ORC circuit is given by:

$$\dot{m}_{ORC} = \dot{m}_{TFC} \left(h_8 - h_5\right) / \left(h_3 - h_{2c}\right) \qquad (8)$$

The specific work of the ORC pump is given by:

$$w_{p,ORC} = v_1 \left(p_{cc,ORC} - p_{con,ORC}\right) / \eta_{p,ORC} \qquad (9)$$

Where $\eta_{p,ORC}$ is the isentropic efficiency of the ORC pump. Energy balance over the IHEX gives:

$$h_{2b} = h_2 + (h_4 - h_{4b}) \qquad (10)$$

Where h_{4b} is the enthalpy of the saturated vapour at the condenser pressure. The enthalpy h_4 is determined by taking into consideration the irreversibility of the turbine as follows:

$$h_4 = h_3 + (h_3 - h_{4s}) \times \eta_t \qquad (11)$$

Where h_{4s} is the enthalpy after an isentropic expansion and η_t is the isentropic efficiency of the turbine. The turbine'sspecific work is then calculated from:

$$w_t = h_3 - h_4 \qquad (12)$$

The thermal efficiency of the ORC circuit alone is given by:

$$\eta_{ORC} = \dot{m}_{ORC}(w_t - w_{p,ORC}) / \dot{Q}_{hs,ORC} \qquad (13)$$

Where $\dot{Q}_{hs,ORC}$ is the heat recovered in ORC circuit, which is given by:

$$\dot{Q}_{hs,ORC} = \dot{m}_{ORC}(h_{2c} - h_{2b}) \qquad (14)$$

The analytical model for the combined cycle

The total heat recovered from the heat source, the total net power produced, and the overall thermal efficiency, respectively, are given by:

$$\dot{Q}_{hs,tot} = \dot{Q}_{hs,TFC} + \dot{Q}_{hs,ORC} \qquad (15)$$

$$\dot{W}_{tot} = \dot{m}_{ORC}(w_t - w_{p,ORC}) + \dot{m}_{TFC}(w_{exp} - w_{p,TFC}) \qquad (16)$$

$$\eta_{tot} = \dot{W}_{tot} / \dot{Q}_{hs,tot} \qquad (17)$$

The overall exergetic efficiency of the combined cycle given by (Yari et al., 2015):

$$\varepsilon_{tot} = \dot{W}_{tot} / \dot{E}_{hs,in} \qquad (18)$$

Where $\dot{E}_{hs,in}$ is the rate of exergy flow of the heat source entering the system as given by:

$$\dot{E}_{hs,in} = \dot{m}_{hs}[(h_{hs,in} - h_0) - T_0(s_{hs,in} - s_0)] \qquad (19)$$

Finally, the temperature of the heat source exiting the system is given by:

$$T_{hs,out} = T_{hs,in} - \dot{Q}_{hs,tot} / \dot{m}_{hs}c_p \qquad (20)$$

Validation of the VBA functions for fluid properties

The Excel-based models developed for the present analyses determine the fluid thermodynamic properties by using the Thermax add-in (El-Awad, 2019). Thermax, which has been developed for educational purposes, provides property functions for ideal gases, saturated water and superheated steam, synthetic and natural refrigerants, psychrometric analyses, two aqua solutions for vapour-absorption refrigeration, combustion and chemically-reacting substances, and air at standard atmospheric pressure. Regarding the functions used in the present analyses, which are those from the refrigerants' group, the functions for saturated liquids and saturated vapours simply interpolate the data given by ASHRAE (2017). For superheated refrigerants, the specific volume is determined by the Redlich-Kwang equation and the enthalpy and entropy are determined by ideal-gas equations in which the specific heat is determined at an adjusted pressure by multiplying the actual pressure by a "compressibility factor" for which an average value of 0.5 is adopted (El-Awad et al. 2019). The use of the adjusted pressure instead of the actual pressure extends the range of these functions to supercritical conditions, but the accuracy of the functions needs to be verified. In what follows, the functions are validated by comparing the results of the model developed for the simple ORC with the data given by Yari et al. (2015).

Figure 2 shows the Excel model developed for the simple ORC by using the data shown on Table 1. The sheet consists of four blocks of cells. The first block on the left side of the sheet stores the specified data, while the second and third blocks in the middle perform the calculations for the ORC model. The fourth block on the right side of the sheet determines the overall parameters that include the total amount of recovered heat (Qhs_tot), the net power produced by the system (Work_net), the exit temperature of the heating source (Ths_out), and the overall energetic and exergetic efficiencies. The sheet uses R152a as the working fluid, but the name of the fluid is stored as a variable so that the model can be used for other fluids.

Pevap f_x =RefPsat_T(Fluid,Tevap)

	A	B	C	D	E	F	G	H	I	J	K	L
1	Fluid	R152a										
2	Heating source (hot water)			Pevap	2342.4	kPa	s4s	2.0198		Q_evap	190.28	kJ/kg
3	Ths_in	120	oC				h4s	515.2144		Q_sensible	79.83881	kJ/kg
4	mflow	100	kg/s	P_cond	909.27	kPa	h4	519.4468		Q_total	270.12	kJ/kg
5	ρ	943.10					x4	0.954475		Q_out	16600.63	kW
6	cp	4.24		h3	543.43					Qhs_tot	18074.17	kW
7				s3	2.0198		T1	40		Work_t	1604.763	kW
8	Tevap	80	oC				h1	271.35		Work_P	131.227	kW
9	T_cond	40	oC	hsat.liq	353.15		v1	0.001163	m3/kg	Work_net	1473.536	kW
10	ΔT_hs2	10.00	K				h2	273.3112		Ths_out	77.41	oC
11				Ths_cc	90.00					therm eff	8.153	%
12	ηt_isen	0.85					s_hs	1.5279		exg eff	25.798	%
13	ηp_isen	0.85		mflowref	66.91	kg/s	s_0	0.3672				
14							Eerg_hs	5711.73				
15	T_0	298.15	K									
16	P_0	101.325	kPa									
17												

Figure 2. The Excel-aided model for the ORC with the data given by Yari et al. (2015)

Table 1. Values of the parameters used for validating the ORC model (Yari et al., 2015)

Parameter	Value
P_0 [kPa]	101.325
T_0 [^{o}C]	25
T_{hs} [^{o}C]	120
$\dot{m}_{hs}$ [kg/s]	100
ΔT_{pp} [K]	10
η_p (%)	85
η_t [%]	85

Yari et al. (2015) developed their model by using the EES software and analysed the cycle's performance with seven working fluids which are: R134a, R1234yf, R152a, propane (R290), n-butane (R600), iso-butane (R600a), and ammonia (R717). The system's power output, thermal efficiency, and exergetic efficiency were calculated at various values of the turbine's inlet temperature, T_3. The results obtained by the present model for the power and thermal and exergetic efficiencies of the same fluids are compared to those obtained by Yari et al. (2015) on Figure 3 and Figure 4. The two figures show that the results obtained by the present model agree well with the results obtained by Yari et al. (2015).

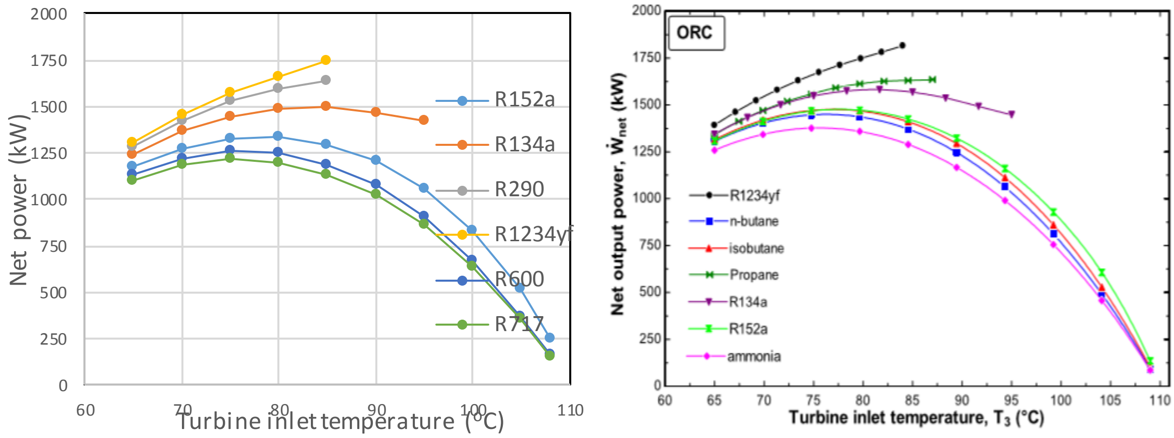

Figure 3. Comparison of (a) the estimations for the present model for the system's power at various values of T_3 with (b) those obtained by Yari et al. (2015)

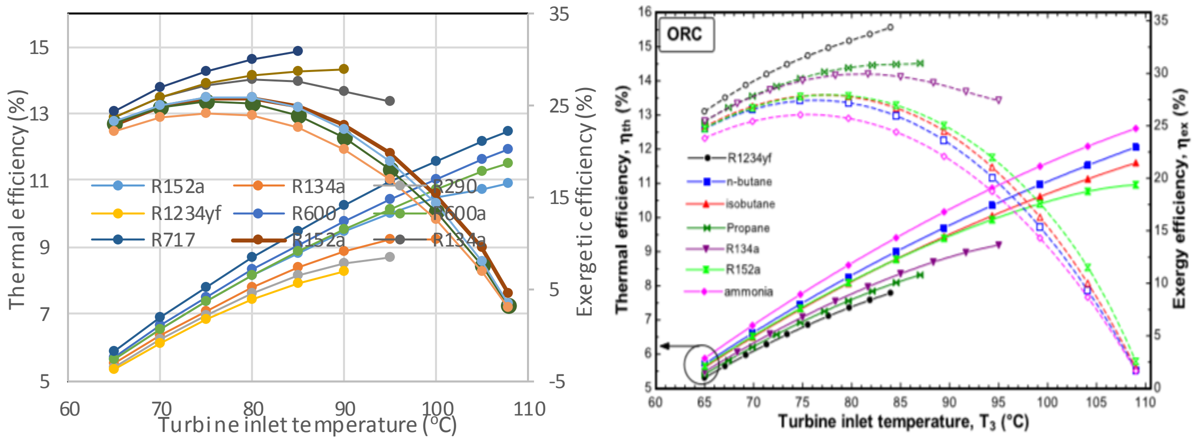

Figure 4. Comparison of (a) the estimations for the present model for the thermal and exergetic efficiencies at various values of T_3 with (b) those obtained by Yari et al. (2015)

RESULTS AND DISCUSSION

Performance of the combined cycle at various cascade temperatures

Figure 5 shows the model developed for the combined cycle in which the first block of cells on the left side of the sheet stores the specified data, while the second and third blocks in the middle perform the calculations for the TFC and ORC circuits, respectively. The names of the working fluids in the TFC and ORC circuits are stored as variables so that the model can be used for different fluid pairs, but R152a is used in both circuits. The model uses the data shown on Table 1 according to which the heat source temperature is 120^{o}C. The temperature of the TFC fluid entering the expander, T_6, is taken as 110^{o}C and the cascade-condenser temperature difference is taken as 3^{o}C. The temperature of the TFC fluid in the cascade condenser is specified as 50^{o}C. By using the model, the cycle's power, thermal efficiency, and exergetic efficiency were calculated at various values of its cascade-condenser temperature and the results are plotted on Figure 6. The figure shows that the power drops as the cascade temperature increases, but the thermal efficiency increases steadily while the exergetic efficiency has an optimum at 75^{o}C. Selecting the appropriate cascade temperature requires a trade-off between the three performance indicators as discussed in the following section.

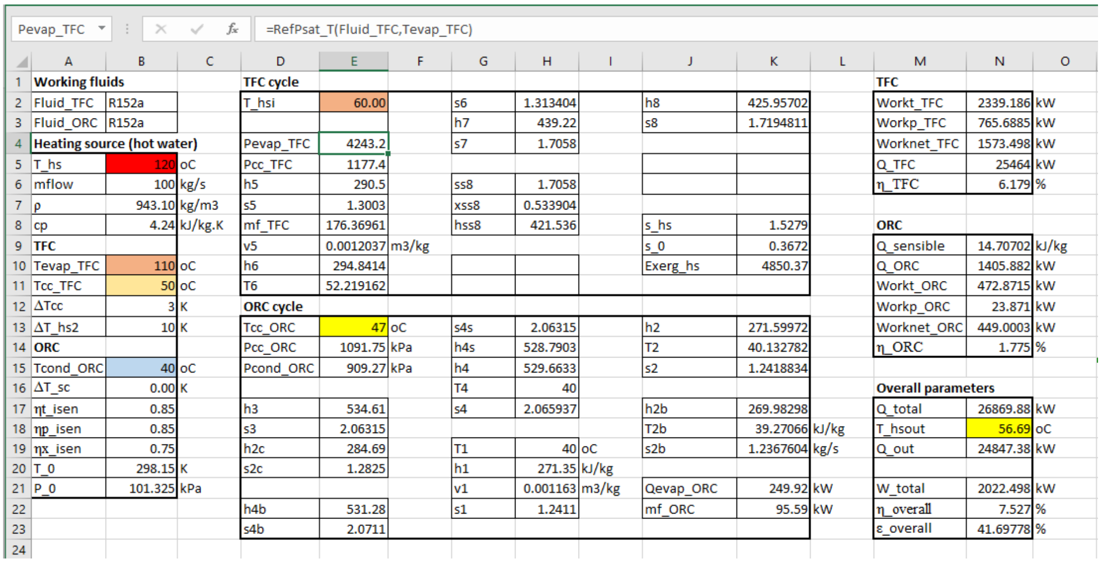

Pevap_TFC =RefPsat_T(Fluid_TFC,Tevap_TFC)

	A	B	C	D	E	F	G	H	I	J	K	L	M	N	O
1	**Working fluids**			**TFC cycle**									**TFC**		
2	Fluid_TFC	R152a		T_hsi	60.00		s6	1.313404		h8	425.95702		Workt_TFC	2339.186	kW
3	Fluid_ORC	R152a					h7	439.22		s8	1.7194811		Workp_TFC	765.6885	kW
4	**Heating source (hot water)**			Pevap_TFC	4243.2		s7	1.7058					Worknet_TFC	1573.498	kW
5	T_hs	120	oC	Pcc_TFC	1177.4								Q_TFC	25464	kW
6	mflow	100	kg/s	h5	290.5		ss8	1.7058					η_TFC	6.179	%
7	ρ	943.10	kg/m3	s5	1.3003		xss8	0.533904							
8	cp	4.24	kJ/kg.K	mf_TFC	176.36961		hss8	421.536		s_hs	1.5279		**ORC**		
9	**TFC**			v5	0.0012037	m3/kg				s_0	0.3672		Q_sensible	14.70702	kJ/kg
10	Tevap_TFC	110	oC	h6	294.8414					Exerg_hs	4850.37		Q_ORC	1405.882	kW
11	Tcc_TFC	50	oC	T6	52.219162								Workt_ORC	472.8715	kW
12	ΔTcc	3	K	**ORC cycle**									Workp_ORC	23.871	kW
13	ΔT_hs2	10	K	Tcc_ORC	47	oC	s4s	2.06315		h2	271.59972		Worknet_ORC	449.0003	kW
14	**ORC**			Pcc_ORC	1091.75	kPa	h4s	528.7903		T2	40.132782		η_ORC	1.775	%
15	Tcond_ORC	40	oC	Pcond_ORC	909.27	kPa	h4	529.6633		s2	1.2418834				
16	ΔT_sc	0.00	K				T4	40					**Overall parameters**		
17	ηt_isen	0.85		h3	534.61		s4	2.065937		h2b	269.98298		Q_total	26869.88	kW
18	ηp_isen	0.85		s3	2.06315					T2b	39.27066	kJ/kg	T_hsout	56.69	oC
19	ηx_isen	0.75		h2c	284.69		T1	40	oC	s2b	1.2367604	kg/s	Q_out	24847.38	kW
20	T_0	298.15	K	s2c	1.2825		h1	271.35	kJ/kg						
21	P_0	101.325	kPa				v1	0.001163	m3/kg	Qevap_ORC	249.92	kW	W_total	2022.498	kW
22				h4b	531.28		s1	1.2411		mf_ORC	95.59	kW	η_overall	7.527	%
23				s4b	2.0711								ε_overall	41.69778	%
24															

Figure 5. Excel-aided model for the combined cycle using R152a

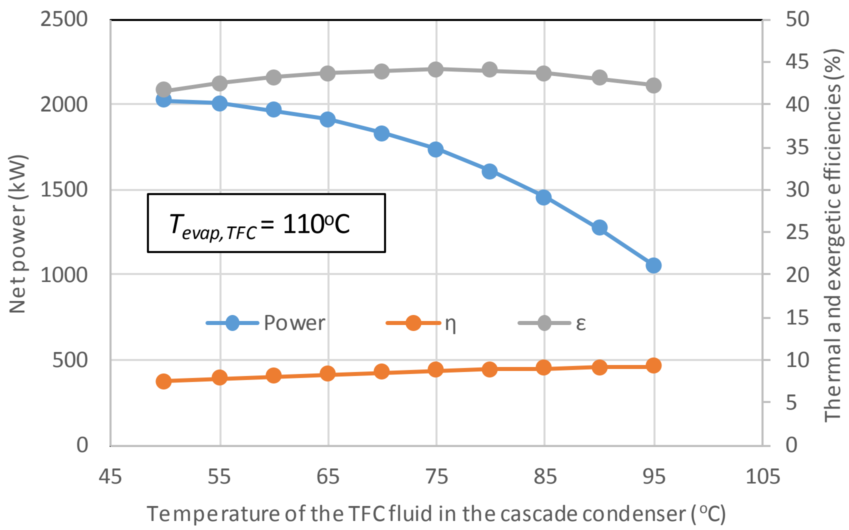

Figure 6. Variation of the combined-cycle's power and thermal and exergetic efficiencies with the temperature of the TFC fluid in the cascade condenser

Tri-objective optimisationof the combined cycle

Determining the cascade temperature that gives the best trade-off between the three cycle's parametersis a tri-objective optimisation problem that requires the cycle's power, thermal efficiency, and exergetic efficiency to be simultaneously maximised. In general, multi-objective optimisation (MOO) analysis can involve other factors such as the economic and environmental factors. While single-objective optimisation analyses can easily be done by using Excel's Solver, MOO analyses require a multi-objective solver. Fortunately, the present analysis involves a single changing variable, which is the temperature in the cascade condenser and, therefore, can be conducted by using the free version of the MIDACO solver (Schlueter et al., 2012) that allows up to four changing variables to be considered. The set-up for MIDACO is shown on Figure 7.

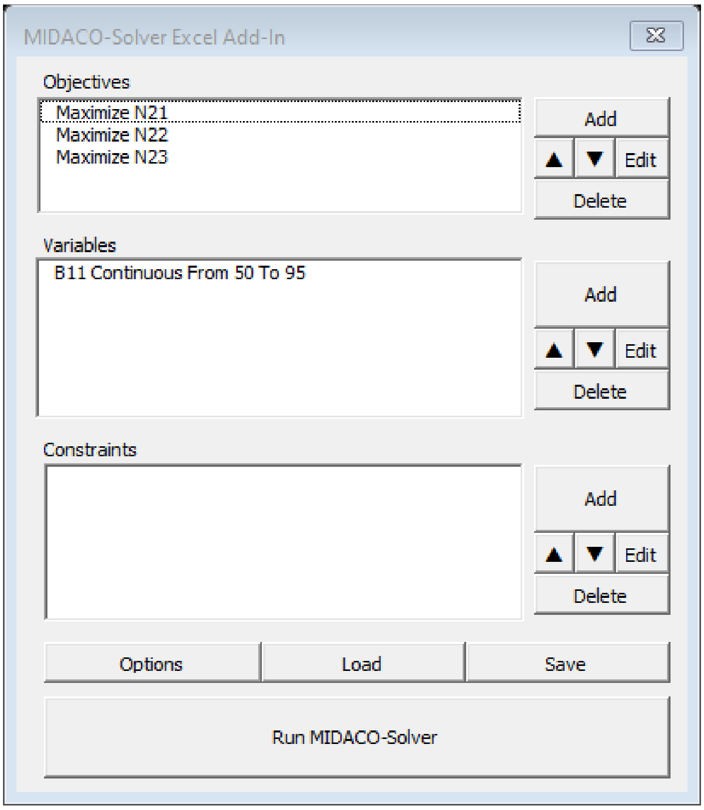

Figure 7. MIDACO's set-up for the dual-objective optimisation of the combined cycle

Three objective functions are involved in the analysis, which are the power, thermal efficiency, and exergetic efficiency of the combined cycle stored in cells N21, N22, and N23 of the model, respectively. All three objectives require the relevant parameter to be maximised by MIDACO by changing a single variable which is the cascade temperature of the fluid used in the TFC circuit stored in cell B10. The lower and upper limits imposed on the changing variable are 50°C and 95°C, respectively. MIDACO and other MOO solvers do not generate a single solution but a Pareto front that contains a set of un-dominated solutions from which one solution is selected. Figure 8 shows the solution selected by MIDACO according to which the temperature of the cascade condenser is 72.83°C.

Pevap_TFC =RefPsat_T(Fluid_TFC,Tevap_TFC)

	A	B	C	D	E	F	G	H	I	J	K	L	M	N	O
1	**Working fluids**			**TFC cycle**									**TFC**		
2	Fluid_TFC	R152a		T_hsi	82.83		s6	1.446641		h8	432.53072		Workt_TFC	1071.495	kW
3	Fluid_ORC	R152a					h7	439.22		s8	1.7122446		Workp_TFC	558.5776	kW
4	**Heating source (hot water)**			Pevap_TFC	4243.2		s7	1.7058					Worknet_TFC	512.9178	kW
5	T_hs	120	oC	Pcc_TFC	2008.326								Q_TFC	15774.73	kW
6	mflow	100	kg/s	h5	337.25223		ss8	1.7058					η_TFC	3.252	%
7	ρ	943.10	kg/m3	s5	1.4368662		xss8	0.452576							
8	cp	4.24	kJ/kg.K	mf_TFC	160.18105		hss8	430.301		s_hs	1.5279		**ORC**		
9	**TFC**			v5	0.0013263	m3/kg				s_0	0.3672		Q_sensible	65.98475	kJ/kg
10	Tevap_TFC	110	oC	h6	340.7394					Exerg_hs	4041.24		Q_ORC	4760.691	kW
11	Tcc_TFC	72.830523	oC	T6	74.432907								Workt_ORC	1364.762	kW
12	ΔTcc	3	K	**ORC cycle**									Workp_ORC	95.784	kW
13	ΔT_hs2	10	K	Tcc_ORC	69.830523	oC	s4s	2.035337		h2	272.6776		Worknet_ORC	1268.978	kW
14	**ORC**			Pcc_ORC	1879.4091	kPa	h4s	520.0802		T2	40.702639		η_ORC	6.338	%
15	Tcond_ORC	40	oC	Pcond_ORC	909.27	kPa	h4	523.4184		s2	1.2452456				
16	ΔT_sc	0.00	K				T4	40					**Overall parameters**		
17	ηt_isen	0.85		h3	542.33441		s4	2.045996		h2b	264.81596		Q_total	20535.42	kW
18	ηp_isen	0.85		s3	2.0353373					T2b	36.508379	kJ/kg	T_hsout	71.61	oC
19	ηx_isen	0.75		h2c	330.80071		T1	40	oC	s2b	1.2203994	kg/s	Q_out	18753.52	kW
20	T_0	298.15	K	s2c	1.4185831		h1	271.35	kJ/kg						
21	P_0	101.325	kPa				v1	0.001163	m3/kg	Qevap_ORC	211.5337	kW	W_total	1781.895	kW
22				h4b	531.28		s1	1.2411		mf_ORC	72.15	kW	η_overall	8.677	%
23				s4b	2.0711								ε_overall	44.0928	%
24															

Figure 8. Performance of the optimised combined cycle with the dual-objective solution obtained by MIDACO

Table 2 compares various key parameters of the optimised solution determined by MIDACO with those of the cycle at the lower and upper limits of the cascade temperature $T_{cc,TFC}$ that yield the maximum power and the maximum thermal efficiency, respectively. The table figures show that the heating source of the optimised solution exits at a temperature of 71.61°C, which is higher than that for the maxmum power but lower than that for the maximum efficiency. Compared to the cycle that gives the maxmimum power, the optimised cycle reduced the rate of recovereed heat by 23.6% and the power by 11.9%, while increasing the exergetic efficiency by 15.3% and the thermal efficiency by 5.7%. Compared to the cycle that gives the maxmimum thermal efficiency, the optimised cycle reduced the thermal efficiency by only 5.9%, but increased the power by 68.8% and the exergetic efficiency by 4.3%. Determining the most suitable fluid pair for the cycle and the appropriate cascade temperature requires a multi-objective optimisation analysis that also takes into consideration the economic and environmental factors.

Table 2. Comparison of the thermodynamic performance of the optimised combined cycle

	Maximise power	Maximise efficiency	Tri-objective
Cascade temperature for TFC fluid, $T_{cc,TFC}$ (^{o}C)	50	95	72.830
Cascade temperature for ORC fluid, $T_{cc,ORC}$ (^{o}C)	47	92	69.831
Heat-source exit temperature, $T_{hs,out}$ (^{o}C)	56.69	93.04	71.61
Heat rejected, $\dot{Q}_{out}$ (kW)	24847.38	10387.04	18753.52
Heat recovered, $\dot{Q}_{hs,tot}$ (kW)	26869.88	11442.67	20535.42
Total power, $\dot{W}_{net,tot}$ (kW)	2022.498	1055.63	1781.895
Thermal efficiency, η_{tot} (%)	7.527	9.225	8.677
Exergetic efficiency, ε_{tot} (%)	41.698	42.288	44.09

REFERENCES

ASHRAE Handbook–Refrigeration, 2017, American Society of Heating, Refrigerating and Air-Conditioning Engineers, Inc., (SI Edition).

Aspen Plus, Aspen Technology Inc., https://www.aspentech.com/en/products/ engineering/aspen-plus

Bidgoli, AA; Yanagihar, JI, Integration of the Compression Units of the Processing Plant with an Organic Rankin Cycle for Power Generation and Cooling Process, Proceedings of ECOS 2023 - the 36th International Conference on Efficiency, Cost, Optimization, Simulation and Environmental Impact of Energy Systems 25-30 June, 2023, Las Palmas De Gran Canaria, Spain

El-Awad, MM, Multi-objective optimisation of VCR systems by applying TOPSIS to the single-objective solutions obtained with Excel Solver, accepted by The Electronic Journal of Spreadsheets in Education (eJSiE), April 2024

El-Awad, MM; Al Nabhani, M.S; Al Hinai, K.S; Younis, A. 2019. Development and Validation of an Excel Add-In for Determining the Properties of Various Refrigerants, Proceedings of First National Conference on Recent Trends in Applied Science, Engineering and Technology (CASET 2K19), Ipri College of Technology, June 11, 2019.

Fierro, JJ; Hern´andez-G´omez, C; Marenco-Porto CA; Nieto-Londo˜no C; Escudero-Atehortua A; Giraldo M; Jouhara H; Wrobel LC; Exergo-economic comparison of waste heat recovery cycles for a cement industry case study, Energy Conversion and Management: X 13 (2022) 100180

Jiménez-García, JC; Ruiz, A; Pacheco-Reyes, A; Rivera, WA, Comprehensive Review of Organic Rankine Cycles. Processes 2023, 11, 1982. https://doi.org/10.3390/pr11071982

Klein, SA; Alvarado, FL, EES: Engineering equation solver for the Microsoft Windows operating system. F-Chart software, 1992

Lemmon, E; McLinden, M; Huber, M; 2004, NIST Fluid Thermodynamic and Transport Properties-REFPROP, Version 7.0 User's Guide.

Mokarram, HN; Mosaffa, AH. Investigation of the thermoeconomic improvement of integrating enhanced geothermal single flash with transcritical organic Rankine cycle. Energy Convers. Manag. 2020, 213, 112831.

Moran, MJ; Shapiro, HN, Fundamentals of Engineering Thermodynamics, 5th edition, John Wiley, & Sons. Inc. 2006

Najjar, YSH; Qatramez, AE. Energy utilisation in a combined geothermal and organic Rankine power cycles. Int. J. Sustain. Energy 2019, 38, 831–848.

Oko, C.O.C.; and Diemuodeke, E.O., MS Excel spreadsheet add-in for thermodynamic properties and process simulation of R152a, Energy Science and Technology, Vol. 5, No. 2, 2013, pp. 63-69.

Oko, C.O.C.; Deebom, M.M.; and Diemuodeke, E.O., Exergoeconomic analysis of cascaded organic power plant for the Port Harcourt climatic zone, Nigeria, Cogent Engineering (2016), 3: 1227127, http://dx.doi.org/10.1080/23311916.2016.1227127

Schlueter, M; Rueckmann, J; Gerdts, M. A Numerical Study of MIDACO on 100 MINLP Benchmarks, Optimization: A Journal of Mathematical Programming and Operations Research, 61,2012, 7, 873-900.

Skiadopoulos. A; Antonopoulou. C; Atsonios. K; Grammelis. P; Gkountas. A; Bakalis. P; Kosmadakis. G; Manolakos. D; Trilateral Flash Cycle for efficient low temperature solar heat harvesting- A case study, Proceedings of ECOS 2023 - the 36th International Conference on Efficiency, Cost, Optimization, Simulation and Environmental Impact of Energy Systems 25-30 June, 2023, Las Palmas De Gran Canaria, Spain

Trædal, S, Analysis of the Trilateral Flash Cycle for Power Production from Low Temperature Heat Sources. Master's Thesis, Institutt for Energi-ogProsessteknikk, KolbjørnHejes v 1B, Trondheim, 2014.

Wolf, C; Rothuizen, E; Ommen, T; Exergoeconomic Analysis of a Solar Powered ORC using Zeotropic Mixtures for Combined Heat & Power Generation, Proceedings of ECOS 2023 - the 36th International Conference on Efficiency, Cost, Optimization, Simulation and Environmental Impact of Energy Systems 25-30 June, 2023, Las Palmas De Gran Canaria, Spain

Yari, M; Mehr, A.S; Zare, V; Mahmoudi, SMS; Rosen, MA., Exergoeconomic comparison of TLC (trilateral Rankine cycle), ORC (organic Rankine cycle) and Kalina cycle using a low grade heat source, Energy 83 (2015) 712-722